

# A purge and trap integrated microGC platform for chemical identification in aqueous samples†

Cite this: *Analyst*, 2014, **139**, 3384

Muhammad Akbar,<sup>a</sup> Shree Narayanan,<sup>a</sup> Michael Restaino<sup>b</sup> and Masoud Agah<sup>\*a</sup>

The majority of current micro-scale gas chromatography ( $\mu$ GC) systems focus on air sampling to detect volatile organic compounds (VOCs). However, purging the VOCs from a water sample using microsystems is an uncharted territory. Various organic compounds used in everyday life find their way to water bodies. Some of these water organic compounds (WOCs) persist or degrade slowly, threatening not just human existence but also aquatic life. This article reports the first micro-purge extractor ( $\mu$ PE) chip and its integration with a micro-scale gas chromatography ( $\mu$ GC) system for the extraction and analysis of water organic compounds (WOCs) from aqueous samples. The 2 cm  $\times$  3 cm  $\mu$ PE chip contains two inlet and outlet ports and an etched cavity sealed with a Pyrex cover. The aqueous sample is introduced from the top inlet port while a pure inert gas is supplied from the side inlet to purge WOCs from the  $\mu$ PE chip. The outlets are assigned for draining water from the chip and for directing purged WOCs to the micro-thermal preconcentrator ( $\mu$ TPC). The trapped compounds are desorbed from the  $\mu$ TPC by resistive heating using the on-chip heater and temperature sensor, are separated by a 2 m long, 80  $\mu$ m wide, and 250  $\mu$ m deep polydimethylsiloxane (OV-1) coated  $\mu$ GC separation column, and are identified using a micro-thermal conductivity detector ( $\mu$ TCD) monolithically integrated with the column. Our experiments indicate that the combined system is capable of providing rapid chromatographic separation (<1.5 min) for quaternary WOCs namely toluene, tetrachloroethylene (PCE), chlorobenzene and ethylbenzene with a minimum detection concentration of 500 parts-per-billion (ppb) in aqueous samples. The proposed method is a promising development towards the future realization of a miniaturized system for sensitive, on-site and real-time field analysis of organic contaminants in water.

Received 4th February 2014  
Accepted 31st March 2014

DOI: 10.1039/c4an00254g

www.rsc.org/analyst

## Introduction

Volatile organic compounds (VOCs) are emitted by a wide variety of products including solids and liquids.<sup>1</sup> Prolonged exposure to VOCs can cause serious health effects including liver, kidney, and nervous system diseases and can even cause cancer.<sup>2-7</sup> Similar effects have been reported for various aquatic organisms.<sup>8-10</sup> Different analytical techniques for their detection have been reported in the literature.<sup>11-13</sup> Microscale gas chromatography ( $\mu$ GC) provides a better solution with reduced size, low power consumption, and can lead to perform a handheld analysis of complex VOCs.<sup>14,15</sup>  $\mu$ GC systems usually consist of an injector/preconcentrator, a separation column and a detector all developed using micro-electromechanical system (MEMS) technology.<sup>13,16-22</sup>  $\mu$ TPC is one of the important components which allows the trace level detection of VOCs by accumulating them over a period of time. The trapped VOCs are

then released in the form of a concentrated plug through a thermal desorption process. The separation column is coated with a stationary phase to separate the VOCs into individual components for final detection by the detector. Several reports have been published for applications of the  $\mu$ GC system related to homeland security, biomedical diagnostics and real-time environmental analysis.<sup>23-25</sup> On the other hand, the detection of VOCs in aqueous matrices has not received adequate attention among the  $\mu$ GC community due to incompatibility of the system with aqueous matrices.<sup>26</sup> Water is found to saturate the adsorbent in the  $\mu$ TPC by capturing available adsorption sites and also damage most common polymer based stationary phases resulting in changes in the retention time, selectivity and column bleeding. Extinguishing the most widely used flame ionization detector (FID) and a decrease in the sensitivity of electron capture detectors (ECDs) has also been reported.<sup>27,28</sup> The United States Environmental Protection Agency (EPA) has specified a list of water organic compounds (WOCs) with their maximum contamination level (MCL). At levels above the specified MCL (usually in ppb), the presence of WOCs in aqueous media poses serious threat to human and aquatic life as shown in Table 1. The current methods for the identification of WOCs rely on removing them from the aqueous sample prior

<sup>a</sup>VT MEMS Lab, Bradley Department of Electrical and Computer Engineering, Virginia Tech, Blacksburg, Virginia 24061, USA. E-mail: agah@vt.edu

<sup>b</sup>Department of Engineering Science and Mechanics, Virginia Tech, Blacksburg, Virginia 24061, USA

† Electronic supplementary information (ESI) available. See DOI: 10.1039/c4an00254g



Table 1 List of water organic compounds with their originating sources and potential health risks

Contaminants	Potential health effect	Contamination sources	Amount recovered (ng)	Recovery	log( $K_{ow}$ )	MCL
Toluene	Nervous system, liver problems	Petroleum factories	5.7	23%	2.75	1 mg l <sup>-1</sup>
PCE	Liver problems; increased risk of cancer	Discharge from factories and dry cleaners	5.4	18%	2.57	5 µg l <sup>-1</sup>
Chlorobenzene	Liver and kidney problems	Discharge from chemical and agricultural chemical factories	9	25%	2.86	0.1 mg l <sup>-1</sup>
Ethylbenzene	Liver and kidney problems	Petroleum refineries	18.7	38%	3.14	0.7 mg l <sup>-1</sup>

to analysis using a bench-top GC system. These methods include solid-phase micro-extraction (SPME), purge and trap, and hollow fiber membranes. They cannot be used for on-site monitoring of the aqueous sample and rely on transporting the sample to the laboratories. Currently, commercially available FROG-4000TM from Defiant Technologies and Water Analysis Surety Prototype (WASP) from Sandia National Laboratories are capable of performing field analysis of water contamination. Nevertheless, the systems are large, expensive, require a trained technician and rely on the conventional purge and trap mechanism. Thus, there still remains a demand for the development of a light weight, less power hungry, inexpensive independent system capable of extracting and detecting WOCs from aqueous media.

Previously, our group followed the direct injection method for monitoring water contamination. This approach requires additional time for removing the trapped water contents from the µTPC adsorbent (dry purge time).<sup>29</sup> Additionally, we also reported microscale headspace sampling as a possible technique to extract WOCs,<sup>30</sup> however, better sensitivity can be achieved through the purge and trap method.<sup>31</sup> This paper describes fluidic integration of µGC components with our newly developed µPE chip for analyzing WOCs. The results indicate that this hybrid integrated system successfully extracted and separated four WOCs at 500 ppb concentration. This is the first realization of an easily deployable microsystem for on-site water monitoring.

## Method description

### General operation

Fig. 1 shows a block diagram explaining the proposed µGC experimental setup including the µPE for extraction of WOCs from the aqueous sample. The µPE device contains two inlets, one for the aqueous sample to be analyzed and one for a pure inert gas to purge the WOCs. The distribution network for aqueous sample entrance provided at the top of the chip is used to uniformly spread the sample inside the chip. Similarly, the multiple inlets for purging gas are intended to enhance the interaction between two phases (air and water) inside the chip and to facilitate the removal of WOCs from the streaming water. The chip also contains two outlets; one is used for water waste and one for directing the purged WOCs to the trap (µTPC). The outlet for directing WOCs to the µTPC is provided at the top corner of the µPE chip. The setup is operated in two phases namely; (1) the extraction phase and (2) the analysis phase.

During the extraction phase, two microfabricated chips (µPE and µTPC) are connected in a tandem configuration using a valve while the µPE chip is maintained vertically (see the ESIf video) to prevent water from entering into the µTPC chip *via* the air outlet. With the vial connected to the sample inlet, the aqueous solution is introduced into the µPE chip using purified nitrogen. High purity nitrogen gas is supplied through the air inlet of the µPE chip trapping WOCs on the adsorbent surface in the µTPC chip. The analyzed mass is calculated from the sample concentration and the volume of water collected during the purged time. During the analysis phase, the µPE is taken offline and the µTPC is connected in series with the µGC column with the embedded µTCD detector using a six port switching valve. Helium is used as a carrier gas while the outlet of the column is connected to the FID of a commercial Agilent HP7890 GC system for verification purposes. The sensor on the backside of the µTPC is used to monitor the temperature profile of the chip when heated. A voltage applied to the heater on the backside of the µTPC heats it up from room temperature to 150 °C. The desorbed WOCs are separated by the µGC column. A 40 mA current is sourced into a Wheatstone bridge with two resistors of the µTCD in each of its arms. The differential voltage measured across the two resistors enables the detection of WOCs which is fed into a Keithley 2700 and recorded on a LabVIEW program.

### µTPC on-chip sensor calibration

For accurately measuring the temperature reached during the desorption process, the on-chip heater was calibrated by placing the µTPC in a commercial GC oven and measuring the resistance for different temperatures.

### µGC column validation

The efficiency of the coated column was evaluated with the µTCD switched to ON condition by applying an 8.3 V DC voltage. This voltage corresponds to a temperature of 95 °C. This was measured with helium flowing at the operating pressure of 12 psi, similar to the method we have previously reported.<sup>32</sup> The metric commonly used for column performance is height equivalent to a theoretical plate (HETP),

$$\text{HETP} = \frac{L}{N}$$

where  $L$  is the length of the column and  $N$  is the number of theoretical plates in the column.  $N$  is calculated experimentally



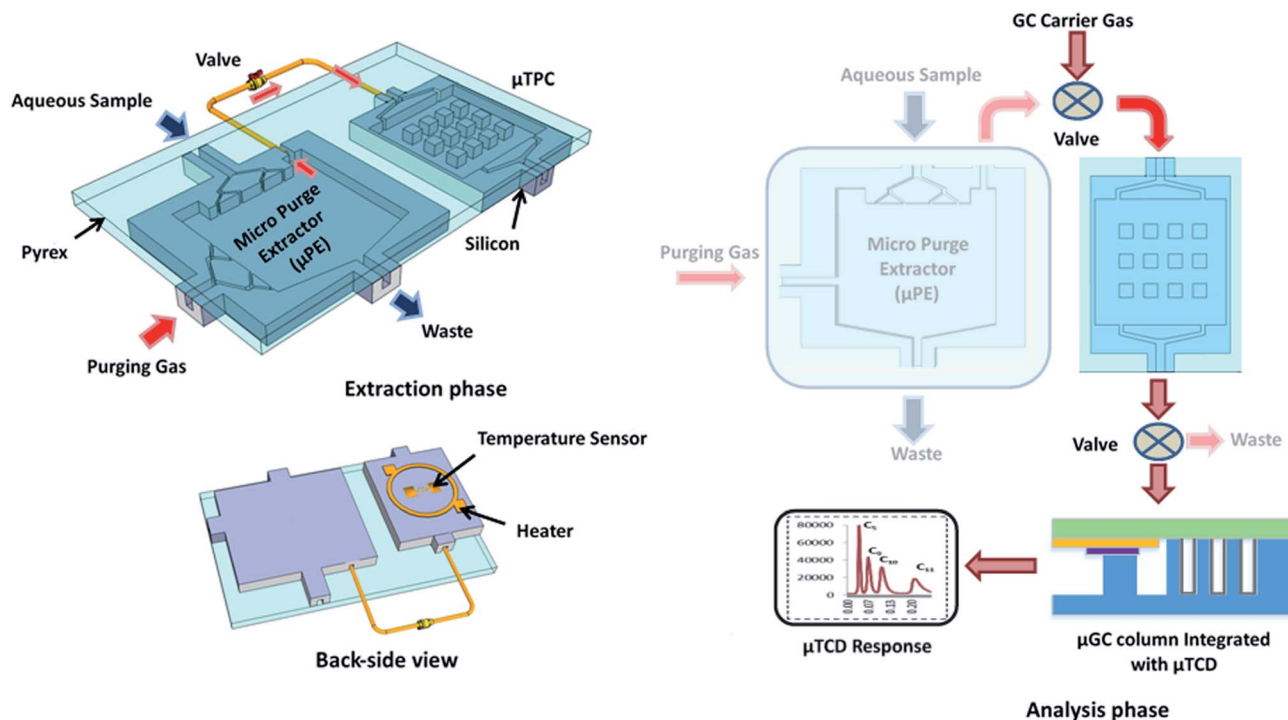


Fig. 1 Conceptual diagram showing the topology for the extraction and analysis of water organic compounds. A back-side heater is utilized for thermal desorption of analytes from the  $\mu$ TPC for chromatographic analysis.

from the peak retention time ( $t_r$ ) and the peak width at half height ( $w_{1/2}$ ).

$$N = 5.54 \left[ \frac{t_r}{w_{1/2}} \right]^2$$

The plate number was calculated over a range of column pressures with the constant split injection ratio of 150 : 1 using chlorobenzene diluted to 2% (v/v) in hexane.

### $\mu$ TCD characterization

The separation and identification of the four WOCs using only the column and its  $\mu$ TCD (without the  $\mu$ PE and  $\mu$ TPC) was performed by installing the chip inside the GC oven with its inlet and outlet connected to the injector and the GC FID, respectively. A 0.1  $\mu$ l volume of the sample containing the WOCs diluted to 2% (v/v) in hexane was injected into the  $\mu$ GC column for separation and identification of the four WOCs by the chip.

Similarly, for  $\mu$ TCD response calibration, five samples (0.5%, 10%, 20%, 30%, and 40% (v/v) in hexane) for each WOC were prepared and tested. A 0.1  $\mu$ l of each sample was injected three times in succession using the GC autosampler module with the split ratio maintained at 150 : 1. By using the density, the mass for each WOC was calculated taking the split injection ratio into account.

## Materials and instruments

Reagent grade WOCs listed in Table 1, solvents, and Tenax TA (80/100 mesh) used in this work were purchased from Sigma-

Aldrich (St. Louis, MO) in >99% purity. AZ9260 photoresist and OV-1 were purchased from MicroChemicals (Germany) and Ohio Valley (Marietta, OH), respectively. Silicon wafers (4 in. dia., 500  $\mu$ m thick, n-type, single side polished) and Borofloat wafers (4 in. dia., 700  $\mu$ m thick, double side polished) were purchased from University Wafers and Coresix Precision Glass (Williamsburg, VA), respectively. Fused capillary tubes (200  $\mu$ m outer dia., and 100  $\mu$ m inner dia.) were purchased from Poly-micro Technologies (Phoenix, AZ).

### Fabrication process

Fig. 2 summarizes the fabrication process for all the three MEMS components. We have previously reported the fabrication, characterization, and operation of the  $\mu$ TPC and the column integrated with the  $\mu$ TCD.<sup>11,16–21</sup> Herein, we briefly discuss the fabrication of these two components in addition to the fabrication of our newly developed microfabricated purge extractor.

### $\mu$ TPC and $\mu$ PE chip

The fabrication of the  $\mu$ TPC was performed on a standard 4" wafer using MEMS processing technology. First, photolithography was performed to pattern micro-posts/fluidic ports. The wafer was then subjected to deep reactive ion etching (DRIE, Alcatel) to achieve a depth of  $\sim$ 250  $\mu$ m. After stripping the photoresist off the front-side, a 500 nm thick oxide layer was deposited on the backside and the wafer diced into individual chips. The chip was then filled with Tenax TA solution (10 mg ml<sup>-1</sup> in dichloromethane) and allowed to evaporate to deposit a thin film ( $\sim$ 200 nm) of the polymer adsorbent on



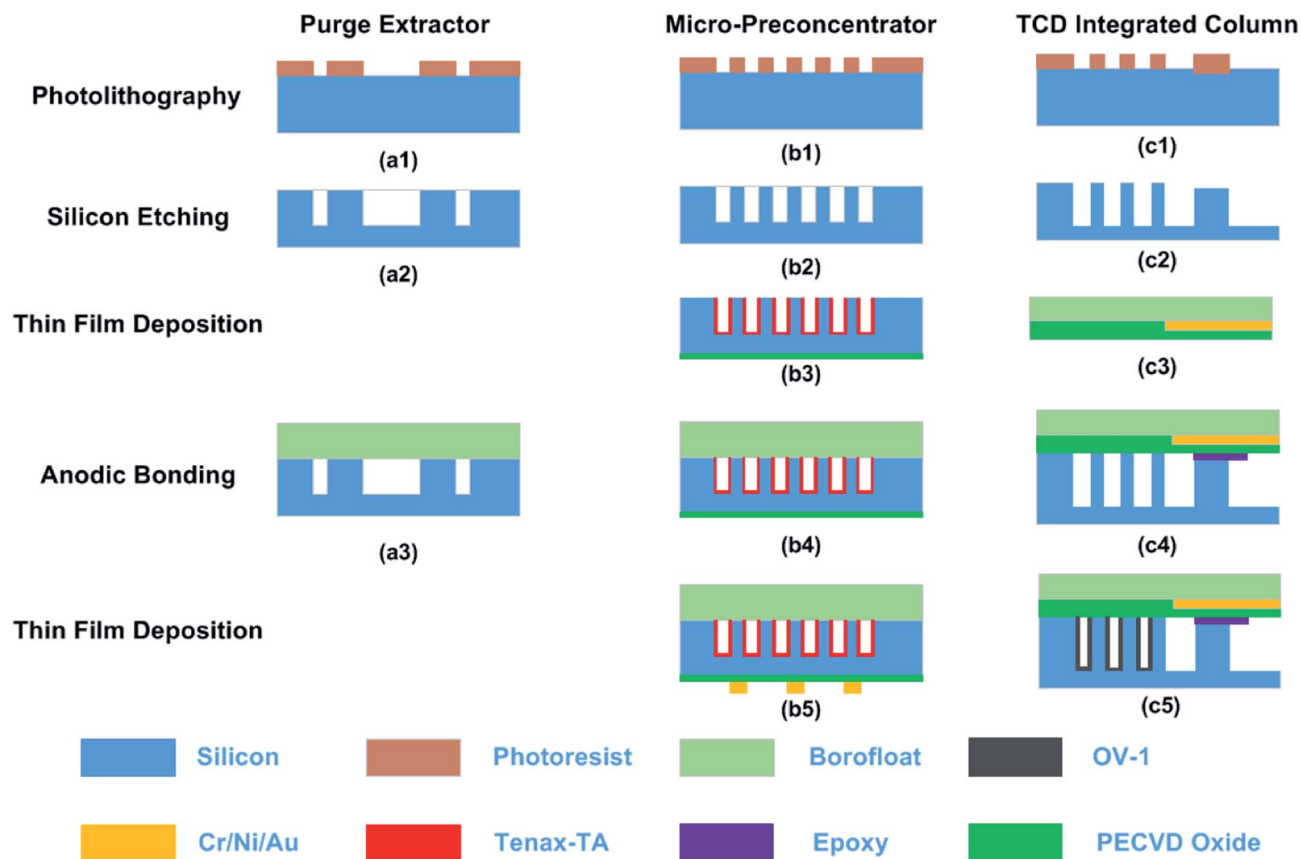


Fig. 2 Fabrication procedure for  $\mu$ PE,  $\mu$ TPC and  $\mu$ GC column with a  $\mu$ TCD detector. The left column shows MEMS processes performed for fabricating these chips.

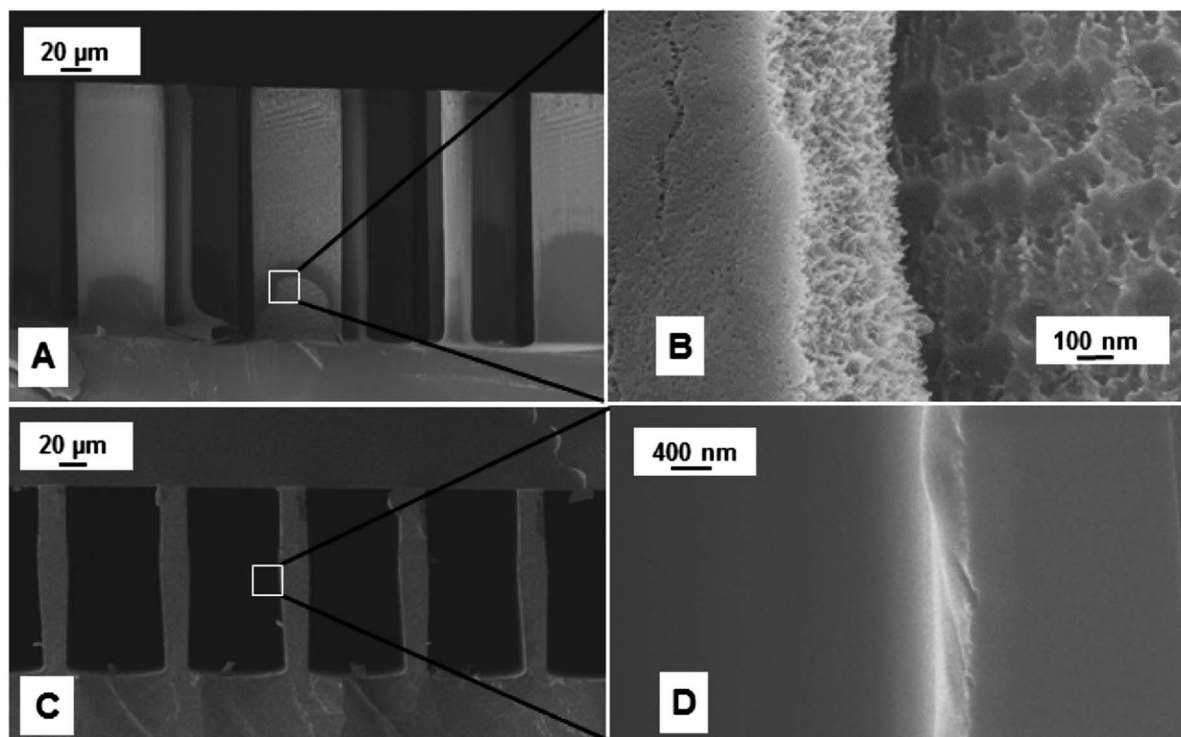


Fig. 3 (A and B) SEM images showing Tenax TA coating on the sidewall of micro-posts inside the  $\mu$ TPC chip, and (C and D) polydimethylsiloxane coating on the interior wall of the column channel.



the cavity surfaces. The chip was then capped with a Borofloat wafer by anodic bonding. Following bonding, the chips were loaded onto the platen of an e-beam evaporator (PVD-250, Kurt Lesker) with the backside facing the crucible. The chips were masked by a stainless steel shadow mask patterned with the features defining the heater and the sensor. Following this, 40 nm/100 nm/25 nm of Cr/Ni/Au was deposited to get nominal resistances of 15 ohm and 250 ohm for the heater and the sensor, respectively. Finally, the devices were unloaded; the shadow masks removed off and fused capillary tubes epoxied into the inlet/outlet ports. The fabrication process of the  $\mu$ PE chip followed that of our  $\mu$ TPC but without the adsorbent coating and backside oxide/metal deposition.

### $\mu$ GC column with embedded TCD

A two-step anisotropic etching of silicon was performed for hosting the feedthroughs and the microfluidic channel by spin coating the wafer with S1813. A shallow depth of 2–3  $\mu$ m was achieved which prevented a contact between the metal interconnects on the Borofloat wafer and the walls of the separation column in silicon upon bonding. A 12  $\mu$ m thick AZ9260 photoresist was patterned with a mask for subsequent deep etching of the channels resulting in 250  $\mu$ m deep channels for the separation. Then, TCD resistors were fabricated on a glass substrate by utilizing a lift-off process of a 40 nm/100 nm/25 nm Cr/Ni/Au stack in the e-beam evaporator. After aligned anodic bonding of the diced detector on glass and the diced separation column on silicon, capillary tubes were epoxied into the inlet/outlet ports. The chip was static coated with polydimethylsiloxane by filling it with a solution of 10 mg ml<sup>-1</sup> OV-1 in pentane, followed by carefully sealing one end with wax and pulling a vacuum at the open end. This procedure left a thin layer of OV-1 coating (~250 nm) on the walls of the column channel. An SEM image of the Tenax TA and OV-1 coating is shown in Fig. 3. The optical image of all fabricated chips is shown in Fig. 4.

### Aqueous sample preparation

To avoid changing the concentration of WOCs, a 24 ml cylindrical vial was filled completely with deionized (DI) water leaving no headspace. Both 1 ppm and 500 ppb solutions (v/v) were prepared in two steps. First, 1000 ppm (v/v) solution was made by adding 24  $\mu$ l of each WOC to 24 ml of DI water. Second, the solution was further diluted 1 : 24 and 1 : 12 with DI water to achieve concentrations of 1 ppm and 500 ppb, respectively. The solution was analyzed immediately to avoid compromising the sample integrity. Before processing any sample, all parts of the equipment in contact with the sample were demonstrated to be interference free. This was accomplished through a blank run.

## Results and discussion

Before evaluating the performance of the whole integrated purge and trap  $\mu$ GC system, the heating and sensing elements of the microfabricated preconcentrator, separation column, and the detector were calibrated and the separation performance of the column was evaluated.

### $\mu$ TPC on-chip heater

A 12 V DC voltage was applied to the heater and the sensor resistance was measured until the resistance representing the desired temperature value was reached. The sensor resistance varied with the applied voltage due to ohmic heating. The final temperature of 150 °C was attained within 7 s representing a ramp rate of 20 °C s<sup>-1</sup>. This condition remained constant during the desorption process of the WOCs trapped on the Tenax TA polymer coating of the  $\mu$ TPC.

### $\mu$ GC column and $\mu$ TCD performance

The maximum plate number (optimum condition) observed for the 2 m long column was about 6200 at 12 psi (flow rate

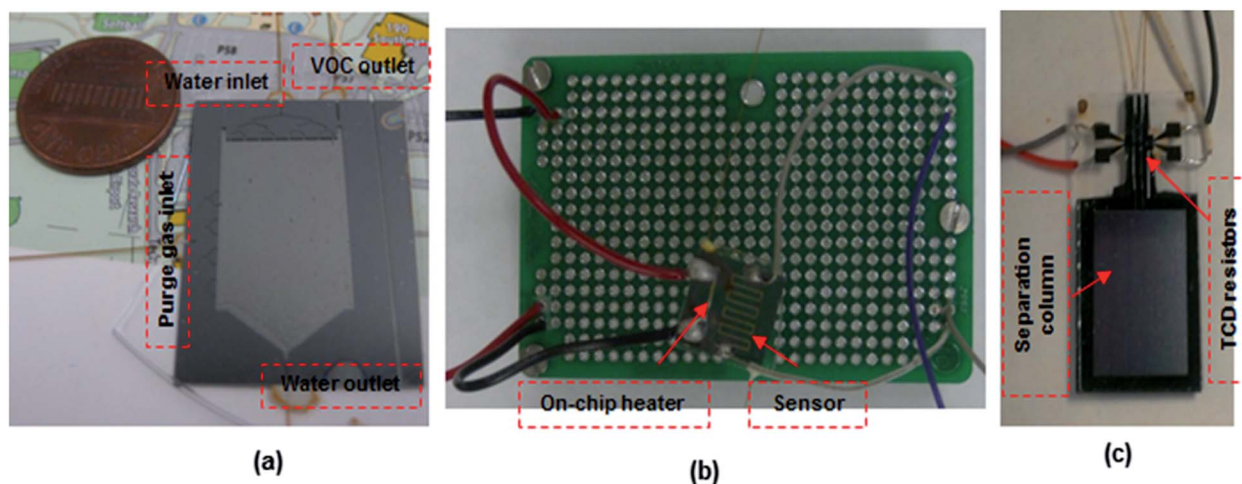


Fig. 4 Optical image of fabricated (a)  $\mu$ PE, (b)  $\mu$ TPC and (c)  $\mu$ GC chip with embedded resistors utilized as the thermal conductivity detector for aqueous analysis.



0.62 ml min<sup>-1</sup>). The column was operating at this optimum flow condition for further investigations.

The separation and identification of the four WOCs was performed by the method described previously. FID was used to verify the chromatogram generated by the  $\mu$ TCD. WOCs were successfully separated and detected by the chip within 1.5 min. Next, a calibration curve showing the output of the  $\mu$ TCD as a function of the injected WOC concentration was obtained by the method described previously. The injected mass varied from about 3 ng to 23 ng for toluene, 5.4 ng to 43 ng for PCE, 3.7 ng to 29.3 ng for chlorobenzene and 3 ng to 23 ng for ethylbenzene. A calibration curve showing the average peak area under the  $\mu$ TCD signal obtained for three injections is shown in Fig. 5. It is worth-mentioning that the conventional TCD has a minimum detection limit of 1 ng.<sup>33</sup> Results obtained indicate a unique response of the  $\mu$ TCD for each WOC with the relative standard deviation (RSD) less than 10% for all cases. The coefficient of determination ( $R^2$ ) was greater than 0.99 in all cases.

### Microsystem evaluation

Following calibration and performance evaluation of each  $\mu$ GC unit, the  $\mu$ PE was put in place. The ability of the complete system comprising  $\mu$ PE and  $\mu$ TPC chips, separation column, and the thermal conductivity gas detector ( $\mu$ TCD) to continuously monitor WOCs in the aqueous sample was realized experimentally by the method explained earlier. The aqueous solution was introduced into the  $\mu$ PE chip using purified nitrogen at 10 psi. High purity nitrogen gas was supplied

through the air inlet of the  $\mu$ PE chip trapping WOCs on the adsorbent surface with a flow rate maintained at 0.4 ml min<sup>-1</sup> (5 psi) through the  $\mu$ TPC chip. The extraction period was varied for three discrete periods of 7, 14 and 21 min. The set of chromatograms in Fig. 6 was generated using 500 ppb and 1 ppm aqueous samples for two different extraction periods. The initial negative dip is due to the sample mixture passing under the reference detector. At this stage, the signal detector experiences the carrier gas and hence is constant. This results in a negative voltage output as explained before.<sup>19</sup> As the sample mixture moves through the column, it is separated over time. When the individual components pass under the sample detector, the reference detector experiences the carrier gas and hence results in positive peaks corresponding to each eluted compound. The second peak is due to trace moisture extracted from the purge chip and is not seen on the FID signal which is insensitive to the trace water content. The increase in peak heights for all WOCs with the increase in extraction time was observed which clearly indicated the validation of the proposed approach. It is also evident that rapid chromatographic separation and detection of all four WOCs within 1.5 min is achieved at room temperature. The method precision was evaluated by three repetitive analyses for each test. After each analysis, the  $\mu$ TCP was heated to 150 °C (conditioning step) to prevent carry-over from the previous runs, following which a blank run was performed to confirm the same. The change in the detector response (area under the peak) with the purge time was then monitored for a sample containing four WOCs at 1 ppm

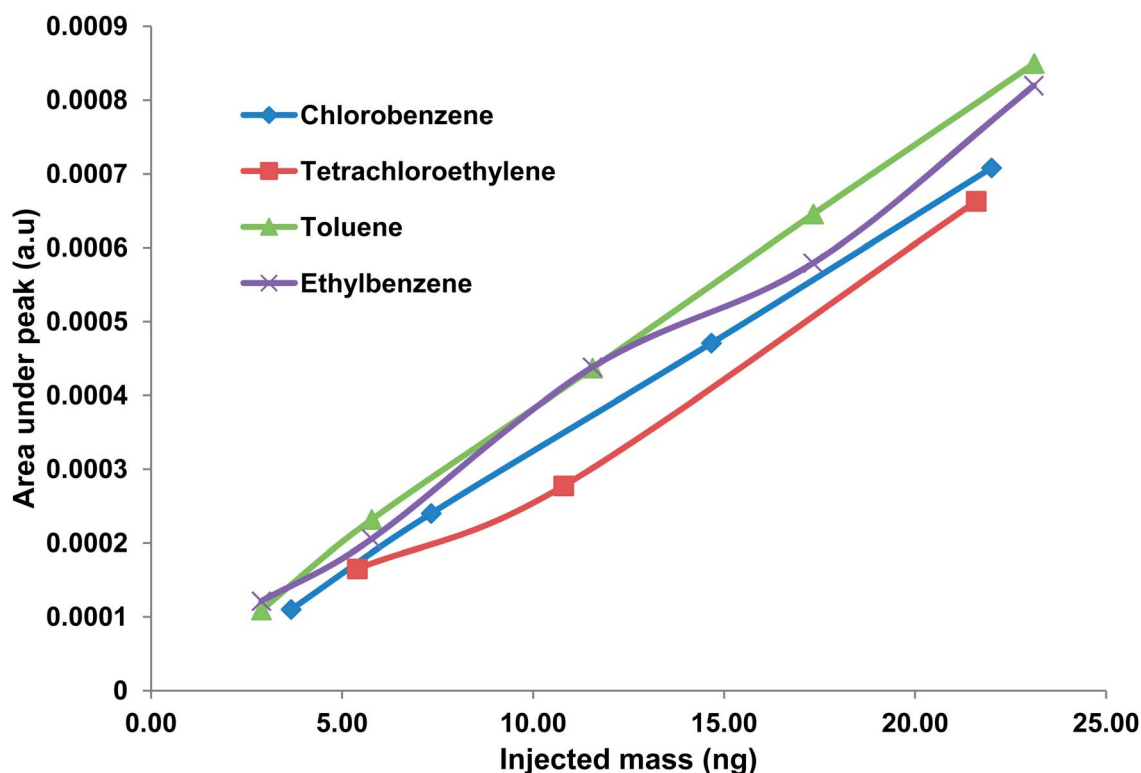


Fig. 5 Calibration curve showing response of  $\mu$ TCD for five different concentrations of WOCs in this study. The relative standard deviation is <10% for all cases. Peak assignments: (1) toluene, (2) tetrachloroethylene, (3) chlorobenzene, and (4) ethylbenzene.



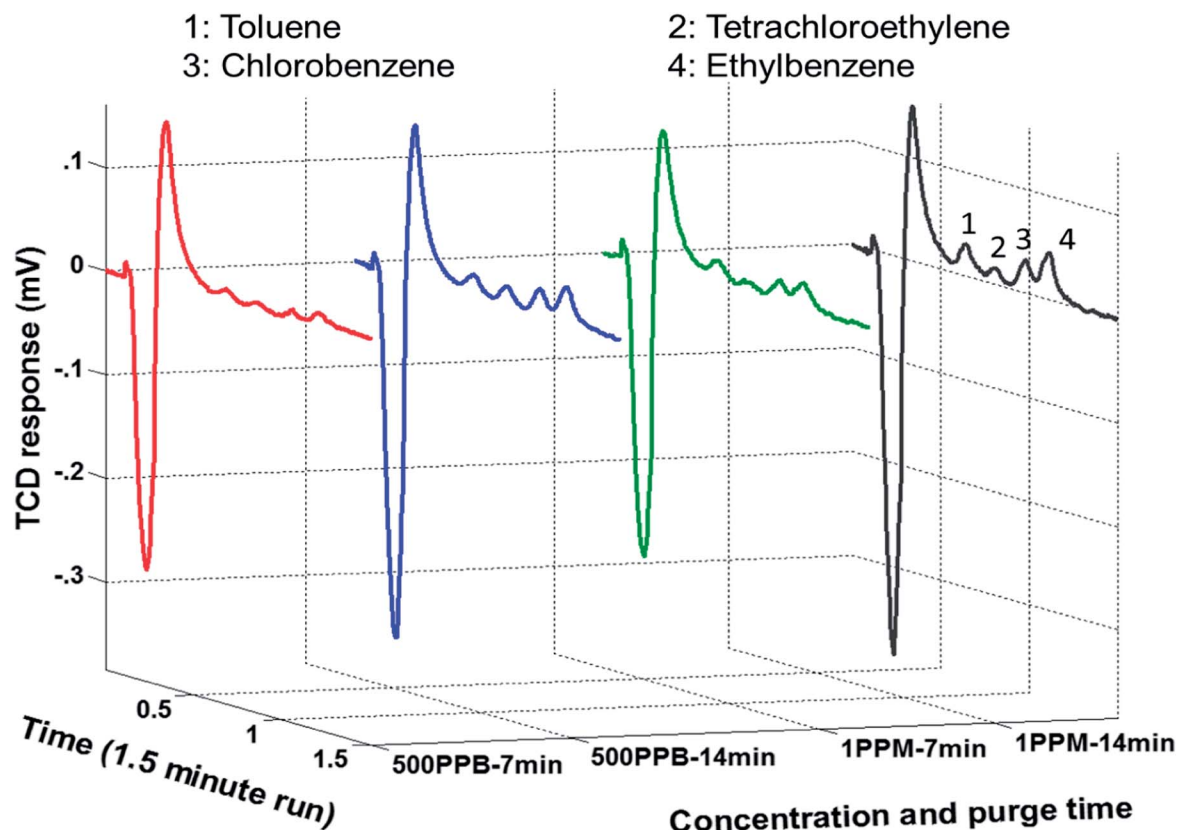


Fig. 6 Set of chromatogram indicating increase in  $\mu$ TCD response with increase in purge time and concentration of WOCs.

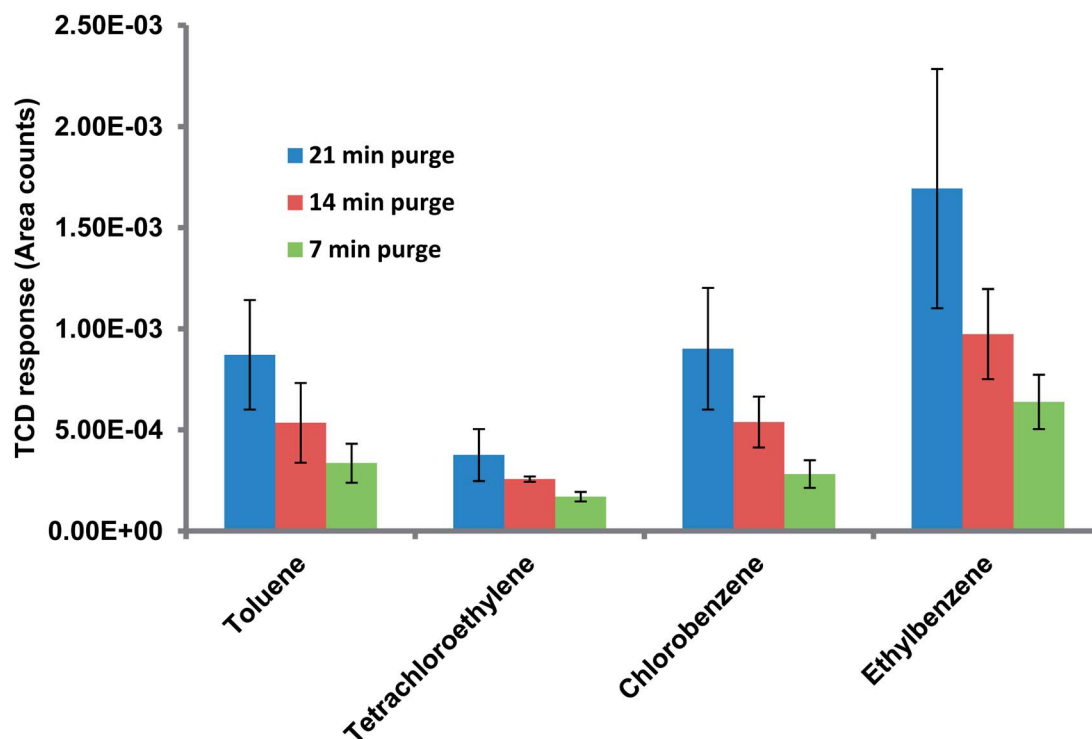


Fig. 7 Graph showing the  $\mu$ TCD response variation with increasing purge time for a sample containing four WOCs at 1 ppm concentration.



concentration. The experiment was repeated thrice for three different purging times and the average value was plotted for each WOC. Fig. 7 shows that the peak area increases with purging time. The increase in the peak area was attributed to the increase in the quantity of nitrogen (inert gas used) that bubbled through the aqueous sample, and consequently, more quantity of WOC moved from the liquid to the vapor phase. Additionally, in streaming mode more fresh sample entered the  $\mu$ PE chip replacing the old one, thereby increasing the amount of WOC purged over time. The results in Fig. 7 indicate that ethylbenzene and chlorobenzene are purged easily from the aqueous sample as compared to PCE and toluene. This is due to their relatively high partition coefficient ( $K_{ow}$ ) value which is defined as the ratio of concentration of a compound in a hydrophobic solvent (usually octanol) to its concentration in water at equilibrium. In other words, it is a measure of hydrophobicity and depends on size, polarity and hydrogen bond strength of a compound. Hydrophilic compounds (with low partition coefficient) are held by a very strong dipole-dipole interaction and hydrogen bond in water and thus could not be easily purged from the sample. Increasing the temperature of the sample should increase the purged amount by supplying enough thermal energy to the molecule to break the dipole-dipole interaction.<sup>34</sup> The sample analyzed during the purge time was collected to determine the percent recovery of each compound. Assuming that the trap is able to capture the entire purged amount, percent recovery is defined as the ratio of the amount that is collected for chromatographic analysis relative to the amount that was originally present in the aqueous sample. Table 1 summarizes the percent recovery for each compound at 1 ppm concentration. The percent recoveries are lower than those reported in the literature.<sup>35,36</sup> This can be attributed to the fact that commercial purge and trap systems use high purging gas flow rates (normally 40 ml min<sup>-1</sup>) and also use traps consisting of a short length micro-bore tubing packed with the granular form of the adsorbent material. Such traps at the cost of high pressure drops and high power consumptions can provide higher adsorption capacity. It is notable that low recoveries have also been reported previously by Sandia National Laboratories in their bench-top (WASP) system described earlier due to the flow limitations in their setup.<sup>37</sup> In addition, we have achieved the detection limit of 500 ppb which is comparatively higher than the commercial purge and trap systems. Part of this is attributed to small sample volumes (in  $\mu$ l) analyzed by the  $\mu$ PE chip when compared to the commercial purge and trap systems. Efforts are underway to improve the extraction efficiency and bring it up to par with the commercial systems. Nevertheless, the purpose of this article is to integrate all  $\mu$ GC components to automate the sampling of water and extract and identify WOCs in real world situations. Modification in design parameters and thermal manipulation for optimization of  $\mu$ PE chip performance will be described in a separate report.

## Conclusions

The first micro-scale version of a purging device for the extraction of WOCs from an aqueous sample has been described. The

potential application of the chip for on-site monitoring of the aqueous sample when equipped with all necessary  $\mu$ GC components has also been discussed. We have first characterized the performance of the  $\mu$ GC column with the  $\mu$ TCD turned ON and explored the optimum conditions for the  $\mu$ GC column. Next, we have obtained a calibration curve indicating the change in  $\mu$ TCD response to different amounts of individual WOCs (in the absence of the  $\mu$ PE and  $\mu$ TPC). We have shown that fixed volume samples of water spiked with known concentrations of the WOCs can be extracted using the  $\mu$ PE chip and subsequently trapped on the  $\mu$ TPC. We have finally determined the percentage recovery of each compound thereby successfully demonstrating the ability of the complete system in analyzing WOCs in an aqueous sample.

We expect to enhance the recovery of analytes by modifying the design of the  $\mu$ PE chip and integrating temperature programming ability on this chip. In future work, in addition to the overall chip size, the design parameters including the location of the inlets and outlets, the configuration of the fluidic ports (distributed *versus* single) and their widths, and the inclusion of pillars and their associated shapes and arrangements will be thoroughly studied to improve the recovery of WOCs. Other parameters including the mode of operation (streaming solution *versus* steady solution), flow rate of the sample to purging gas in streaming mode and temperature manipulation for purging high boiling point organic compounds (semi-VOCs) as external controllable parameters on recovery of WOCs will also be considered.

## Acknowledgements

This research has been supported by the National Science Foundation (NSF) under CAREER Award no. ECCS-0747600 and NIOSH Grant 5R21OH010330. All the FESEM images were taken at Virginia Tech Institute for Critical and Applied Science, Nano Scale Characterization and Fabrication Laboratory (ICTAS-NCFL). Fabrication of the devices was performed at Virginia Tech Microfabrication Cleanroom Facilities.

## Notes and references

- 1 U. E. Oswer, *Draft Guidance for Evaluating the Vapor Intrusion to Indoor Air Pathway from Groundwater and Soils (Subsurface Vapor Intrusion Guidance)*, US Environmental Protection Agency, 2002.
- 2 K. S. Betts, *Environ. Health Perspect.*, 2010, **118**, A173.
- 3 P. Burkhardt-Holm, T. Wahli and W. Meier, *Ecotoxicol. Environ. Saf.*, 2000, **46**, 34–40.
- 4 P. A. Jones, V. A. Baker, A. J. E. Irwin and L. K. Earl, *Toxicol. in Vitro*, 1998, **12**, 373–382.
- 5 T. Nishihara, J. Nishikawa, T. Kanayama, F. Dakeyama, K. Saito, M. Imagawa, S. Takatori, Y. Kitagawa, S. Hori and U. Hideo, *J. Health Sci.*, 2000, **46**, 282–298.
- 6 D. Pobel, E. Riboli, J. Cornée, H. Bertrand and M. Guyader, *Eur. J. Epidemiol.*, 1995, **11**, 67–73.
- 7 S. R. Corporation and C. Associates, *Toxicological Profile for N-nitrosodimethylamine*, 1989, p. 755.





- 8 H. Ishibashi, M. Hirano, N. Matsumura, N. Watanabe, Y. Takao and K. Arizono, *Chemosphere*, 2006, **65**, 1019–1026.
- 9 M. F. Kirby, A. J. Smith, J. Rooke, P. Neall, A. P. Scott and I. Katsiadaki, *Aquat. Toxicol.*, 2007, **81**, 233–244.
- 10 F. Lahnsteiner, B. Berger, F. Grubinger and T. Weismann, *Aquat. Toxicol.*, 2005, **71**, 297–306.
- 11 B. Alfeeli, V. Jain, R. K. Johnson, F. L. Beyer, J. R. Heflin and M. Agah, *Microchem. J.*, 2011, **98**, 240–245.
- 12 J. J. Johnston, D. A. Goldade, D. J. Kohler and J. L. Cummings, *Environ. Sci. Technol.*, 2000, **34**, 1856–1861.
- 13 C.-J. Lu, W. H. Steinecker, W.-C. Tian, M. C. Oborny, J. M. Nichols, M. Agah, J. A. Potkay, H. K. L. Chan, J. Driscoll, R. D. Sacks, K. D. Wise, S. W. Pang and E. T. Zellers, *Lab Chip*, 2005, **5**, 1123–1131.
- 14 W. R. Collin, G. Serrano, L. K. Wright, H. Chang, N. Nuñovero and E. T. Zellers, *Anal. Chem.*, 2013, **86**, 655–663.
- 15 J. H. Seo, J. Liu, X. Fan and K. Kurabayashi, *Lab Chip*, 2013, **13**, 851–859.
- 16 M. Akbar and M. Agah, *J. Microelectromech. Syst.*, 2013, **22**, 443–451.
- 17 M. Akbar, D. Wang, R. Goodman, A. Hoover, G. Rice, J. R. Heflin and M. Agah, *J. Chromatogr. A*, 2013, **1322**, 1–7.
- 18 M. Akbar, D. Wang, H. Shakeel, J. R. Heflin and M. Agah, *The 17th International Conference on Solid-State Sensors, Actuators and Microsystems: Transducers & Eurosensors XXVII*, 2013.
- 19 S. Narayanan, B. Alfeeli and M. Agah, *IEEE Sens. J.*, 2012, **12**, 1893–1900.
- 20 H. Shakeel and M. Agah, *J. Microelectromech. Syst.*, 2013, **22**, 62–70.
- 21 D. Wang, H. Shakeel, J. Lovette, G. W. Rice, J. R. Heflin and M. Agah, *Anal. Chem.*, 2013, **85**, 8135–8141.
- 22 T. Sukaew, H. Chang, G. Serrano and E. T. Zellers, *Analyst*, 2011, **136**, 1664–1674.
- 23 S. K. Kim, H. Chang and E. T. Zellers, *Anal. Chem.*, 2011, **83**, 7198–7206.
- 24 J. H. Seo, S. K. Kim, E. T. Zellers and K. Kurabayashi, *Lab Chip*, 2012, **12**, 717–724.
- 25 J. H. Seo, J. Liu, X. Fan and K. Kurabayashi, *Anal. Chem.*, 2012, **84**, 6336–6340.
- 26 E. R. Kuhn, *LCGC North Am.*, 2002, **20**, 474–478.
- 27 K. Grob and A. Habich, *J. High Resolut. Chromatogr.*, 1983, **6**, 11–15.
- 28 U. R. Bernier, C. L. Bray and R. A. Yost, *J. Microcolumn Sep.*, 2000, **12**, 226–235.
- 29 B. Alfeeli and M. Agah, *14th International Conference on Miniaturized Systems for Chemistry and Life Sciences*, 2010, 1721–1723.
- 30 M. Akbar and M. Agah, *IEEE Sensors*, 2012, 915–918.
- 31 M. Careri, G. Mori, M. Musci and P. Viaroli, *J. Chromatogr. A*, 1999, **848**, 327–335.
- 32 S. Narayanan and M. Agah, *J. Microelectromech. Syst.*, 2013, **22**, 1166–1173.
- 33 H. M. McNair and J. M. Miller, *Basic gas chromatography*, John Wiley & Sons, 2011.
- 34 C.-W. Lee and C. P. Weisel, *J. Anal. Toxicol.*, 1998, **22**, 1–5.
- 35 E. Martínez, S. I. Lacorte, I. Llobet, P. Viana and D. Barceló, *J. Chromatogr. A*, 2002, **959**, 181–190.
- 36 J. M. Warner and R. K. Beasley, *Anal. Chem.*, 1984, **56**, 1953–1956.
- 37 A. N. Irwin, C. D. Mowry and T. T. Borek III, *Research into the variables affecting purge and trap collection for a portable field trihalomethane testing unit*, 2006, 1–32.

